Cellulose Film with Air Barrier and Moisture-Conducting Character Fabricated by a Green Process

Junwu Peng
Wuhan Textile University - Yangguang Campus: Wuhan Textile University
Yanan Li
Wuhan Textile University - Yangguang Campus: Wuhan Textile University
Xinglin Liu
Wuhan Textile University - Yangguang Campus: Wuhan Textile University
Guizhen Ke
Wuhan Textile University - Yangguang Campus: Wuhan Textile University
Dengpeng Song
Wuhan Textile University - Yangguang Campus: Wuhan Textile University
Shuangquan Wu
Wuhan University Zhongnan Hospital
Weilin Xu
Wuhan Textile University - Yangguang Campus: Wuhan Textile University
Kunkun Zhu (kkzhu@wtu.edu.cn)
Wuhan Textile University - Yangguang Campus: Wuhan Textile University

Research Article

Keywords: cellulose, NMMO, air barrier, moisture-conducting

Posted Date: July 8th, 2021

DOI: https://doi.org/10.21203/rs.3.rs-656845/v1

Abstract

The use of nature polymer to prepare degradable films is a sustainable production concept that can improve resource utilization and reduce the environmental pollution caused by traditional packaging waste or another field. Here, a regenerated cellulose film was prepared through the N-methylmorpholine-N-oxide (NMMO) cellulose system. The most critical peculiarity is that films with air barrier and moisture conduction character, because the surface of film is dense and does not allow small molecules like oxygen to pass through, but water molecules can move freely in the film by means of hydrogen bonds. This shows that the cellulose film has in textiles, food preservation, medicine and other fields. Significantly, the film has good tensile strength (maximum strength reaches 149.5 MPa) and light transmittance (more than 80% at 600 nm). Moreover, the effect of coagulation bath concentration, temperature and the content of glycerin on film strength was discussed.

Introduction

In recent years, non-renewable resources have gradually been exhausted, and petroleum-based products are increasingly polluting the environment. Green energy conservation has inevitably become the mainstream of the times. Therefore, it is necessary to explore renewable natural polymer materials to replace traditional industrial petroleum-based polymers for materials fabrication. Cellulose, the most important component of natural polymers, has considerable output on the earth as more than 180 billion tons of production each year (Raghuwanshi et al., 2019). It is a superb ideal to use cellulose for materials preparation instead of petroleum-based polymers. However, cellulose is difficult to dissolve, because there are a large number of hydrogen bonds exists in the molecule together with the rigid molecular chain conformation. These hydrogen bonds form a tightly packed grid, give the cellulose very stable characteristics (Alexandridis et al., 2018; Rabideau et al., 2015; Mao et al., 2010). In previous studies, researchers have developed many cellulose solvent systems, including N-methylmorpholine-N-oxide (NMMO), ionic liquid (IL), lithium chloride/N,N-dimethylacetamide (LiCl/DMAc), sodium hydroxide aqueous solution system, alkali/urea system, tetrabutylammonium fluoride/dimethyl sulfoxide system, metal complex solution, etc. (Yuan et al., 2018; J. Duan et al., 2015; Trygg et al., 2011; YukinobuFukaya et al., 2008; Samir et al., 2005; Heinze et al., 2005; Swatloski et al., 2002; Matsumoto et al., 2001; Heinze et al., 2000). The discovery of these solvents has greatly promoted the application and development of cellulose. Among the many solvents mentioned above that can be used to dissolve cellulose, NMMO is defined as a green, non-toxic, environmentally friendly and economical cellulose solvent.

A thin film is a layer of material ranging from fractions of a nanometer to several micrometers in thickness, has been increasingly applied in diverse fields, such as separation, chemicals, pharmaceuticals, food, textiles, biomedicine, etc. (Xie et al., 2021; Nunes et al., 2020; Xu et al., 2018; Yang Zhang et al., 2018). However, the preparation of thin film materials in the traditional sense usually uses petroleum-based as the basic raw material. In addition, a large number of toxic organic solvents are involved in the processing (Xie et al., 2021). Although this kind of film can meet the production requirements, its further development is restricted due to their non-degradability and unsustainability

production process. So, it is imperative to improve the sustainability of the films and the green transformation of the production process. Therefore, the films prepared using cellulose as a raw material or cellulose as a matrix material through green solvents have received widespread attention (Y. Qi et al., 2021; Wan et al., 2021; Yu Zhang et al., 2020; L. Zhang et al., 2013). In this work, cellulose films with air barrier and moisture-conducting character were prepared from NMMO solvent through a casting mothed. These films exhibited high strength (149.5MPa), good transmittance (80% at 600nm), low cytotoxicity and good biocompatibility. This work provides a reference for the sustainable development of the film production industry while expanding the application range of cellulose.

Experimental

Materials

NMMO was purchased from the Jinao Chemical Company of Anhui as a dried 97 wt% solid powder. The cellulose, cotton linter short pulp, $M\eta=10.0\times10^4$, Hubei Jinhuan New Material Technology Co., Ltd. The glycerine was purchased from Sinopharm Chemical Reagent Co., China and used without further purifications.

Dissolution of cellulose

The aqueous solution containing NMMO (87 wt%) was used as solvent of cellulose. To prepare the cellulose solution, cotton linter pulp in the desired amount was dispersed into the NMMO solvent preheated to 100 ^{o}C with mechanical stirring (900 rpm). After 2.5 hours, the cotton pulp was dissolved, and a pure and sticky relatively cellulose solution was obtained after centrifugation at 8000 rpm for 30 seconds at 15 ^{o}C.

Preparation of cellulose films

The cellulose solution, after removal of air bubbles, was spread on a glass plate, which is preheated to 80 ^{o}C, and then immersed in regenerated solution (water) at low temperature to get the cellulose hydrogels with thickness of 0.4 mm. The resulted hydrogels were washed with distilled water to remove any residuals, and then fixed on an organic(Polymethyl methacrylate) glass plate(PMMA) to air-dry at ambient temperature to form dry films (with thickness of 0.16 mm). The cellulose films were coded as CL-N0, CL-N2.5, CL-N5, CL-N7.5, CL-N10, corresponding to regenerating in water with 0 wt%, 2.5 wt%, 5 wt%, 7.5 wt% and 10 wt% NMMO. Another series of cellulose films were regenerated in 0 wt% NMMO aqueous solution, which coded as CL-T0, CL-T20, CL-T40 and CL-T60 by changing the regenerating temperature of 0 ^{o}C, 20 ^{o}C, 40 ^{o}C and 60 ^{o}C. In addition, in the process of preparing CL-N0 films, a series of completely washed CL-N0 hydrogels is selected, the hydrogels were immersed into glycerin solution for 1h to give cellulose hydrogels. By changing the content of glycerin solution such as 0 wt%, 2 wt%, 5 wt%, 10 wt%, a series of cellulose soaked in glycerin were obtain. Then, fixed on organic glass plate to air-dry at ambient temperature to form dry films coded as CL-G0, CL-G2, CL-G5, CL-G10.

Characterization

Using the ultraviolet-visible-near-infrared spectrophotometer (UV-3600 Plus, Shimadzu Ltd., Japan), the light transmittance of the sample is measured in the range of wavenumber 800-200 cm^{-1}. FT-IR spectra of these samples were recorded via a Nicolet FT-IR spectrometer (FT-IR, Nicolet 6700, Shimadzu Ltd., Japan).

Thermal stability test. Thermal gravimetric analysis (TGA, SDTQ500, TA Instrument Ltd., US.) was carried out by using a thermo-gravimetric analysis.

X-ray Diffraction. After the sample is cut as much as possible, the X-ray diffraction spectrum of the sample is measured at room temperature within the range of 5-45° with the Empyrean intelligent X-ray diffractometer from PANalytical, Holland. Refer to the method of Bingbing Zheng and BB(B. Zheng et al., 2017; Yuping et al., 2010), the crystallinity of CL-NX films was determined using Jade 6.0 software according to the following equation

$$X=\sum I_C / (\sum I_C+\sum I_a)$$

Where $\sum I_C$ is the integral intensity of total polycrystal diffraction of crystalline portion while $\sum I_a$ is the scattering integral intensity of amorphous portion.

Mechanical properties and Scanning Electron Microscope (SEM). The cross section of the CL-N series film was sputtered with gold, observed by SEM (Phenom pure, Fu Na Scientific Instruments (Shanghai) Co., Ltd., Shanghai, China) at 10 KV and the mechanical properties of all films were measured by a universal testing machine (Testing Machines, 5943, INSTRON Ltd., US.).

In Vitro Cell Assay. The CCK-8method is used to evaluate cell compatibility, in this experiment, NIH-3T3 cells was used and cultured in Dulbecco's modified Eagle's medium (DMEM) supplemented with 10% fetal bovine serum (FBS) and 1% streptomycin/penicillin at 37 ℃ under a humidified atmosphere with 5% CO_2.

The clean CL-N series films (CL-N0, CL-N2.5, CL-N5, CL-N7.5, CL-N10) were cut and grinded into powder, respectively, and placed into PBS solution to obtain a 500μg/ml sample suspensions of different films. Then, NIH-3T3 cells was seeded in 96-well plates with 4×10^3 cells per well and cultured to adhere at 37 °C for 24 h in 5% CO_2 atmosphere. 50μL samples suspension were added into plates and cultured with cells at 37 °C for 24 h and 72 h, the equal volume of PBS without samples was as a control. To evaluate the viability, the media was replaced by 200 μL of culture medium with 10% CCK-8 (Cell Counting Kit-8, Dojindo Laboratories, Japan) and further incubated for 4 h at 37 °C. Then 150 μL supernatant liquid incubated media were transferred to fresh 96-well plates for colorimetric assessment using a microplate reader at 450 nm. Cell viability was calculated using the flowing formula:

$$\text{Cell viability (\%)} = (A_{test} - A_0) / (A_{control} - A_0) \times 100$$

Where the A_{test} and the $A_{control}$ were the absorbance of the experimental groups and the control group, A_0 was the absorbance of CCK8 in culture medium without cells. The data of sextuplicate samples are expressed as mean ± the standard deviation (SD).

Biological Compatibility of CL-N series films.

The cells cultured with films were stained by Calcein-AM (green, live) / PI (red, dead) kit to evaluate the biological compatibility of the CL-N series films. 1 mL fresh NIH-3T3 cells suspension (2.5×10^4 cells/mL) were seeded in 24-well plates, 300 μL samples suspension were added in and cocultured with NIH-3T3 cells at 37 °C for 24h and 72h, the culture medium without samples was as a control group. After being washed again with PBS, 200 μL Calcein-AM / PI solution (5 μL Calcein-AM and 15 μL PI in 5 mL PBS) was added in plate wells with an incubation for 20 min at 37 °C, then the stained cells were washed with PBS and immediately observed by a fluorescence microscope at the corresponding excitation wavelength (490±10 nm).

Air barrier and moisture-conducting function test. The CL-G2 film was prepared in the experiment and divided into two groups: an apple group and a color-changing silica gel group. In the apple group, the cut apple strips are put into a sample bottle filled with nitrogen, the first sample bottle is sealed with PE film, the second sample bottle is sealed with CL-G2 film, and the last one is unsealed (kept in contact with the air). The mass of each sample bottle is obtained by the electronic balance, and then it is allowed to stand at a temperature of 24 ^{o}C and a relative humidity of 51%. During the standing period, the apple status and the quality change of the sample bottle are continuously observed (time interval is 1 h). In the color-changing silica gel group, the experimental method and conditions are consistent with the apple group, except that the apple pulp strips in the sample bottle are replaced with color-changing silica gel.

Discussion And Result

Preparation process of cellulose film. Figure 1a shows the fabrication process and formation mechanism of the cellulose films. Cellulose cotton pulp was dispersed in 87 wt% NMMO aqueous solution at 100 ^{o}C under mechanical stirring. The oxygen atom of NMMO molecular can form hydrogen bonds with the hydroxyl of cellulose to destroy the crystalline structure of cellulose and results in a clear homogeneous solution where the polymer chains are molecularly isolated(Sayyed et al., 2019). After high-speed centrifugation to remove bubbles in the solution, the cellulose solution is coated on a glass plate, and finally immersed in a water bath. During in the regeneration process, the NMMO molecular diffused from the NMMO-cellulose system into water, then the cellulose chains aggregated together to form hydrogel. The resulting hydrogel was washed with water to remove residual chemicals, and then fixed on a polymethyl methacrylate (PMMA) plate to dry at room temperature, then a flexible and transparent cellulose film was obtained (Fig. 1b).

Characteristics of CL-N series films. As shown in Fig. 2a, the CL-N series film has satisfactory transparency, the transmittance of all film is above 80% at the wavelength range of 490-780nm.

Expressly, CL-N0 film has the highest transmittance (87% at 550 nm), this transparency is comparable with that of commercial regenerated films (Wan et al., 2021). At the same time, the content of NMMO in the coagulation bath have a certain effect on the transparency of the cellulose film that transmittance of the film decreased with the increase of the NMMO content in the coagulation bath, which can be explained by the film formation mechanism of the phase inversion (Ilyas et al., 2021; Cheng et al., 1995; Cheng et al., 1994). As the concentration of the coagulation bath increases, the delay time of the system increases, and the polymer concentration at the film/coagulation bath interface decreases. The film surface layer is more likely to undergo phase separation, such that the porous cellulose hydrogel is formed (Reuvers, van den Berg, et al., 1987; Reuvers & Smolders, 1987). When light travels through such a structure, multiple reflections and refractions will occur, and part of the light will even be depleted in the end. The macroscopic manifestation is that the light transmittance of the film decreases (Shahbazi et al., 2019; Gobrecht et al., 2015; Tang et al., 2008). Figure 2b shows the FTIR spectrum of the CL-N series films. Both CL-N0 and other films show characteristic peaks of cellulose, E.g. 3442 cm^{-1}(O-H, v), 2902 cm^{-1}(C-H, v_{as}), 1374 cm^{-1}(C-O-H, δ), and 897 cm^{-1}(C-O-C at the β-(1–4)-glycosidic linkage, v_{as}) (Shandilya et al., 2020). The characteristic peaks of NMMO at 2935 cm^{-1}(C-H, v), 1448 cm^{-1}(C-H_2, δ), 1116 cm^{-1}(C-O-C, v), and 858 cm^{-1}(C-O-C, δ) are not observed in the spectra, suggesting that there is no chemical reaction occurred between the NMMO and cellulose(Yu Zhang et al., 2020). Figure 2c shows the TG and DTG test curves of the CL-N series film. The decomposition temperature of all samples is almost the same, including that the use of different concentrations of NMMO in coagulation bath does not affect the thermal stability of the films. Figure 2d shows the X-ray diffraction images of cellulose film of CL-N0, CL-N2.5, CL-N5, CL-N7.5, CL-N10, respectively. According to the method of Zheng, Bingbing et al.(B. Zheng et al., 2017), The relative crystallinity calculated by Jade 6.0 software is found to be about 24.23%, 26.86%, 27.60%, 54.34%, and 62.67% for CL-N0, CL-N2.5, CL-N5, CL-7.5, CL-N10 film, respectively. These results indicating that the NMMO in coagulation bath is helpful for the formation of cellulose crystals. The NMMO concentration difference between cellulose solution and coagulation bath, reduced with the increase of NMMO content, the double diffusion rate between the solvent and the nonsolvent decreased, thus the cellulose molecules have enough time to rearrange and crystallize (Ichwan et al., 2012; Yaopeng Zhang, 2002; Bang et al., 1999; van de Witte et al., 1996).

Cross-section morphology of CL-N series films. Based on the picture in Fig. 3, it was found that the film is clearly divided into two areas with different densities and the pore size is decrease when the NMMO content in coagulation bath temperature increases from 0 (water only) to 10 wt % NMMO. The formation of two areas in films is due to the unlike exchange rate of different part in coagulation bath. On the side where the solution is in contact with PMMA plate, the film is denser since there is less chance of contact with the coagulation bath and the slower exchange rate compare with another side. As the concentration of the coagulation bath to rise, the exchange rate between another side and the side in contact with PMMA plate to decrease, and finally a uniform and dense film is formed. The formation of a pore can be explained by Laity, P. R and Muhammad Ichwan's, work (Ichwan & Son, 2012; Laity et al., 2002). In P.R. Laity's work, the coagulation process of film was summarized into four route (phase separation occurs in the □) vitrification region, □) the metastable region between the binodal and spinodal lines, □) the unstable

region, □) metastable region) according to the locations on the phase diagram where the phase separation takes place and the corresponding morphologies. This film is considered as result of the nucleation growth mechanism as demonstrated by routes □ above for the slow solidification process and the uniform dense structure as shown in Fig. 3b-f. When the cellulose/NMMO aqueous solution is immersed into NMMO/H_2O (coagulation bath), liquid–liquid phase separation occurs between cellulose solution and coagulation bath. Then, as when entering the metastable region between binodal and spinodal line, nuclei are formed in the polymer solution, these nuclei grow into droplets until their growth is stopped by the solidification of the surrounding polymer solutions. Finally, the pore structure of films was formed (Lee et al., 1999). In this case, nuclei have enough time to grow up due to the low exchange rate of NMMO and water and finally form homogenous and dense film. Therefore, addition of NMMO to coagulation bath will slower the diffusion rate and allow nuclei to grow homogenously to yield denser and smaller pore size of film structure with the content of NMMO increase.

Mechanical property of cellulose films under different preparation conditions. In this study, the effects of different coagulation bath concentrations, coagulation bath temperature, and glycerin on the strength of the film were discussed. The mechanical strength test results of all films as show in Fig. 4a-c. and Fig. 4a shows results of the mechanical test of CL-N series film, which is regenerated under different concentrations of NMMO in coagulation bath. With the increase of NMMO content from 0–10%, the tensile strength of the cellulose film increased from 106.1MPa to 149.5MPa, higher than the regeneration cellulose film fabricated in alkali/urea system (Fig. 4d, Table 1)(Shi et al., 2019). This is because the cellulose film was prepared with different concentrations of the coagulation bath results in different degrees of crystallinity (Fig. 2d). It is worth mentioning that the post-treatment of glycerin and the regeneration temperature of the film also have some influence on its mechanical properties. As shown in Fig. 4b, the tensile strength of the CL-G series film, which is treated with different glycerin concentrations, will decrease. Compared with CL-G0 film, the tensile strength of CL-G2 film has dropped to 61.5MPa, a decrease of 0.6 times, but the elongation at break of CL-G0 film, is 4.3%, and the CL-G2 film is 7.3%, an increase of nearly 0.6 times, similar with the chitin films (B. Duan et al., 2014). This can be explained that the glycerol molecule act as a plasticizer in the cellulose film for its small molecule relative to the cellulose molecule. Specifically, the glycerol molecule penetrates into the gaps between the cellulose molecules when the cellulose hydrogel film is soaking in the glycerin solution, which weaken the cellulose molecular chain, and made the cellulose molecule chains easier to slip (Jianqing et al., 2008). Therefore, the tensile strength of the cellulose film treated with glycerol will decrease while the elongation at break will increase. At the same time, the glycerin concentration used to treat the cellulose hydrogel should not be too large. Experiments show that when the glycerin concentration reaches 5 %, the corresponding tensile strength of the CL-G5 film drops to an unfavorable value. Similar to the effect of glycerin on the films, the increase in regeneration temperature also reduces the tensile strength of the film to a certain extent. Figure 4c is a stress-strain curve for testing the mechanical properties of CL-T0, CL-T20, CL-T40, and CL-T60 films. The tensile strength of the film decreases only when the temperature rises from 0 ^{o}C to 20 ^{o}C. Compared with the CL-G series of film, the elongation at break of CL-T0, CL-T20, CL-T40, and CL-T60 film decreases correspondingly with the increase of regeneration temperature, this is because as the

regeneration temperature increases, the thermal movement of molecules intensifies, the diffusion speed of NMMO molecules in the coagulation bath is accelerated, and the precipitation and reorganization of cellulose molecules are also accelerated, which is not conducive to the formation and growth of cellulose crystals (Yaopeng et al., 2002), and because of the loss of the lubrication effect of the glycerin molecule, the elongation at break of the cellulose film has also decreased. In general, increasing the concentration of coagulation bath or temperature will reduce the strength of the cellulose film, while the addition of plasticizers (such as glycerin) can significantly increase the toughness of the films. Therefore, the strength of the film can be adjusted by changing concentration and temperature of coagulation bath during the preparation of films. At the same time, plasticizer can be added to adjust the toughness during the post-treatment of films. Finally, considering the amount of plasticizer, concentration and temperature of coagulation bath, cellulose films with different strength characteristics can be obtained.

Table 1
Mechanical property of CL-N series film compared with other regenerated cellulose films.

Solvent	Classification	Stress (MPa)	Strain (%)	Thickness (um)	Ref
NMMO	Organic solvents	106.3-149.5	4.1-6.0	16 ± 2	This work
NMMO	Organic solvents	82.3 ± 10.6	10.7 ± 2.0	30	(Kim et al., 2011; Mao et al., 2010; Khare et al., 2007)
		64.9 ± 18.3	6.5 ± 1.5	14 ± 0.5	
		73.1 ± 10.1	15.8 ± 1.3	25	
CA(cellulose acetate)	Acid	60.1 ± 11.6	13.1 ± 8.0	/	(Khare et al., 2007)
[DBNH][OAc]	IL (Ionic Liquids)	188	2.9	/	(Niu et al., 2021)
1-Allyl-3-methylimidazolium chloride ([Amim][Cl])	IL (Ionic Liquids)	160	20	/	(Wan et al., 2021; X. Zheng et al., 2019; Yan et al., 2016)
		152 ± 30	/	/	
		208 ± 7.1	5.5 ± 0.9	/	
1-ethyl-3-methylimidazolium acetate [Emim][Ac]	IL (Ionic Liquids)	100–110	7.5-8	/	(Pang et al., 2015)
Benzyl trimethyl ammonium hydroxide (BzMe3NOH)	Alkali	158.3 ± 0.7	21.6 ± 1.9		(Y. Wang et al., 2019)
NaOH/urea	Alkali/urea	129 ± 10	1.44	/	(Liu T, 2012)
		90 ± 5	1.85		
		97 ± 3	3.53		
		100 ± 5	2.96		
		89 ± 4	3.27		
		105 ± 6	8.14		
NaOH/urea	Alkali/urea	87	9–10	20	(H. Qi et al., 2009)

Solvent	Classification	Stress (MPa)	Strain (%)	Thickness (um)	Ref
LiOH/urea	Alkali/urea	86.9	6–7	/	(Shi et al., 2019; Liu et al., 2019; C. Wang et al., 2018)
		50–60	4–5	/	
		66.5	16.5	/	

Solvent resistance test of CL-N0. To prove chemical stability of the cellulose film, the solvent resistance test of CL-N0 film was carried out and the results shows in Fig. 5. Even after immersing in acid (pH = 1), alkali (pH = 14) and other solvency for 24 hours, it can still maintain its original shape. It is shows that the cellulose film is chemically inert to a variety of solvents, this is because the hydrogen bonds between the cellulose molecular chains that make up films have strong interactions. Hence it is very difficult for common solvents to destroy this structure. This feature can ensure that the film remains stable in complex chemical environment. In fact, composite films based on cellulose and chitosan films with similar structures have the same excellent performance in solvent resistance experiments (Shi et al., 2019; Zhu et al., 2019). In these works, films in different solvents only show swelling and its geometry has not been destroyed.

Cytotoxicity and biological compatibility evaluation of CL-N series films. In this work, the in vitro cytotoxicity and biocompatibility tests were carried out by a direct contact of NIH-3T3 cells with CL-N series films for 1d and 3d. The cell proliferation was evaluated by CCK-8 assay and the live-dead cells were stained by Calcein-AM / PI kit. In Fig. 6a, it can be found that the cell viability of all groups is higher than 95 % compared to that of control group both in 1d and 3d culture incubation. This result revealed that the CL-N series films had no side effect and cytotoxicity on cell proliferation. This conclusion was further evidenced by fluorescence microscope images (Fig. 6b), in which NIH-3T3 cells was live–dead stained with the green color standing for live cells and the red color standing for dead cells. It's shown that there are no obvious dead cells in both CL-N series films group and control groups, the cell number all had a fast increase from 1d to 3d incubation and the morphology are all similar fibroblast-like, indicating that cells could be alive and continuously grew with good cell adhesion in the existence of CL-N series films, confirming the good biocompatibility of the cellulose films prepared by NMMO, which is consistent with the chemical crosslinked cellulose film(Shi et al., 2019). Therefore, it's providing experimental support for potential application of cellulose in food preservation and textiles field.

The moisture-conducting and air barrier properties of the cellulose film. Air barrier and breathable materials have been widely used in warm cotton clothing, wound dressings, medical dressings and food packaging (Yue et al., 2021; Zhou et al., 2021; Patil et al., 2020; Tehrani-Bagha et al., 2019; Hu et al., 2006). In order to measure the air and moisture-conducting character of the cellulose film, CL-G2 film was used as a representative sample to air barrier and moisture-conducting function test, the results are shown in Fig. 7a. In the apple experiment, with the extension of the test time, it can be observed that the

color of apple of the CL-G2 film group and the PE film group was still bright, while the apples in the blank group have become dull and brown due to oxidation. In the PE group, the flesh is slightly yellowed due to loss of water. This shows that the fiber prepared in the laboratory has the same function of isolating oxygen as the PE film on the market. The test results of the film moisture-conducting character are shown in Fig. 7a. With the extension of the test time, the silica gel in the blank group and the CL-G2 group began to fade, while the color of the silica gel in the PE film group hardly changed. At the same time, the quality change of apple and silica gel in the sample bottle also proved this, in Fig. 7b, it can be clearly observed that the quality of apple and silica gel in the blank group and CL-G2 group has changed, while the PE group remains stable. As show in Fig. 7c, gas such as oxygen and carbon dioxide cannot pass through the film, because of the dense surface. But due to the hydrophilicity of cellulose film, water molecules can form hydrogen bonds with the cellulose chains and conduct from one side (high relative humidity) of the film to another side (low relative humidity). Finally, carbon dioxide is accumulated on one side, so the film has a certain carbon dioxide control function. In food storage, gas permeable membrane with suitable H_2O permeation could maintain an atmosphere with low O_2 concentration and high CO_2 concentration, which restrains plants physiological metabolism to a low degree, inhibits the proliferation of bacteria, and finally effectively extend the storage time of food (Zhou et al., 2021). And as textile, the film can be used as the middle layer to compound with other fabrics to prepare moisture-permeable and wind-proof work clothes.

Conclusion

A series of cellulose films were prepared using the NMMO/H_2O system, the maximum tensile strength can reach 149.5MPa (CL-N10), and the maximum elongation at break can reach 28.5% (CL-G10), the film prepared in the laboratory has good thermal stability, resistant to strong acid and alkali corrosion, stable in a variety of organic solvents, the survival rate of cells cultured on the CL-N series cellulose dry film is higher than 95%, no cytotoxicity, and the cells on the dry film showed good reproductive ability, which makes the cellulose film have application potential in the medical field. Critically, the cellulose film has the function of preventing air and moisture-conducting, which is very important in the fields of clothing, food packaging, and medical dressings.

Declarations

Author Information

Corresponding Authors

* E-mail: kgz66@126.com (Ke, G.)

Shuangquanwu@wtu.edu.cn (Wu, S.)

kkzhu@wtu.edu.cn (Zhu, K.)

Funding: This work was supported by the National Natural Science Foundation of China (22005226), Hubei Provincial Department of Education Science and Technology Research Program (204013)

Conflict of interest: The authors declare that they have no known competing financial interests or personal relationships that could have appeared to influence the work reported in this paper. All the authors listed have approved the manuscript enclosed.

Ethical statement: All authors state that they adhere to the Ethical Responsibilities of Authors. In addition, the work is compliance with ethical standards.

References

1. Alexandridis, P., Ghasemi, M., Furlani, E. P., & Tsianou, M. (2018). Solvent processing of cellulose for effective bioresource utilization. *Current Opinion in Green and Sustainable Chemistry,* 14, 40-52. https://doi.org/10.1016/j.cogsc.2018.05.008
2. Bang, Y. H., Lee, S., Park, J. B., & Cho, H. H. (1999). Effect of coagulation conditions on fine structure of regenerated cellulosic films made from cellulose/N-methylmorpholine-N-oxide/H_2O systems. *Journal of Applied Polymer Science,* 73(13), 2681-2690. 10.1002/(SICI)1097-4628(19990923)73:13
3. Cheng, L.-P., Dwan, A.-H., & Gryte, C. C. (1995). Membrane formation by isothermal precipitation in polyamide-formic acid-water systems II. Precipitation dynamics. *Journal of Polymer Science Part B: Polymer Physics,* 33(2), 223-235. https://doi.org/10.1002/polb.1995.090330207
4. Cheng, L.-P., Soh, Y., Dwan, A. H., & Gryte, C. (1994). An Improved Model for Mass Transfer During the Formation of Polymeric Membranes by the Immersion-Precipitation Process. *Journal of Polymer Science Part B: Polymer Physics,* 32, 1413-1425. 10.1002/polb.1994.090320813
5. Duan, B., Chang, C., & Na, N. (2014). Structure and Properties of Films Fabricated from Chitin Solution by Coagulating with Heating. *Journal of Applied Polymer Science,* 131. 10.1002/app.39538
6. Duan, J., Liang, X., Cao, Y., Wang, S., & Zhang, L. (2015). High Strength Chitosan Hydrogels with Biocompatibility via New Avenue Based on Constructing Nanofibrous Architecture. *Macromolecules,* 48(8), 2706-2714. 10.1021/acs.macromol.5b00117

7. Gobrecht, A., Bendoula, R., Roger, J.-M., & Bellon-Maurel, V. (2015). Combining linear polarization spectroscopy and the Representative Layer Theory to measure the Beer–Lambert law absorbance of highly scattering materials. *Analytica Chimica Acta,* 853, 486-494. https://doi.org/10.1016/j.aca.2014.10.014
8. Heinze, T., Dicke, R., Koschella, A., Kull, A. H., Klohr, E.-A., & Koch, W. (2000). Effective preparation of cellulose derivatives in a new simple cellulose solvent. *Macromolecular Chemistry and Physics,* 201(6), 627-631. https://doi.org/10.1002/(SICI)1521-3935(20000301)201:6
9. Heinze, T., & Koschella, A. (2005). Solvents applied in the field of cellulose chemistry: a mini review. *Polímeros,* 15(2), 84-90. 10.1590/S0104-14282005000200005
10. Hu, J., & Mondal, S. (2006). *9 - Study of shape memory polymer films for breathable textiles*. In H. R. Mattila (Ed.), *Intelligent Textiles and Clothing* (pp. 143-164): Woodhead Publishing
11. Ichwan, M., & Son, T.-W. (2012). Preparation and characterization of dense cellulose film for membrane application. *Journal of Applied Polymer Science,* 124(2), 1409-1418. https://doi.org/10.1002/app.35104
12. Ilyas, A., Yihdego Gebreyohannes, A., Qian, J., Reynaerts, D., Kuhn, S., & Vankelecom, I. F. J. (2021). Micro-patterned membranes prepared via modified phase inversion: Effect of modified interface on water fluxes and organic fouling. *Journal of Colloid and Interface Science,* 585, 490-504. https://doi.org/10.1016/j.jcis.2020.10.031
13. Jianqing, W., & Li, Z. (2008). Preparation of Cellulose Films and Mechanical Properties by NMMO. *Journal of Tianjin University of Science and Technology,* 23(04), 9-13.
14. Khare, V. P., Greenberg, A. R., Kelley, S. S., Pilath, H., Juhn Roh, I., & Tyber, J. (2007). Synthesis and characterization of dense and porous cellulose films. *Journal of Applied Polymer Science,* 105(3), 1228-1236. https://doi.org/10.1002/app.25888
15. Kim, C.-J., Khan, W., Kim, D.-H., Cho, K.-S., & Park, S.-Y. (2011). Graphene oxide/cellulose composite using NMMO monohydrate. *Carbohydrate Polymers,* 86(2), 903-909. https://doi.org/10.1016/j.carbpol.2011.05.041
16. Laity, P. R., Glover, P. M., & Hay, J. N. (2002). Composition and phase changes observed by magnetic resonance imaging during non-solvent induced coagulation of cellulose. *Polymer,* 43(22), 5827-5837. https://doi.org/10.1016/S0032-3861(02)00531-1
17. Lee, S., Kim, J., & Lee, C.-H. (1999). Analysis of $CaSO_4$ scale formation mechanism in various nanofiltration modules. *Journal of Membrane Science,* 163(1), 63-74. https://doi.org/10.1016/S0376-7388(99)00156-8
18. Liu T, L. Z., Song C, Hu Y, Han Z, She J, Fan F, Wang J, Jin C, Chang J, Zhou JM, Chai J. (2012). Chitin-induced dimerization activates a plant immune receptor. *Science,* 336(6085), 1160-1164.
19. Liu, Y., Xu, S., Jing, M., Wei, Y., Deng, H., & Fu, Q. (2019). Preparation of high-performance cellulose composite membranes from LiOH/urea solvent system. *Nanocomposites,* 5(2), 49-60. 10.1080/20550324.2019.1619962

20. Mao, Z., Cao, Y., Jie, X., Kang, G., Zhou, M., & Yuan, Q. (2010). Dehydration of isopropanol–water mixtures using a novel cellulose membrane prepared from cellulose/N-methylmorpholine-N-oxide/H_2O solution. *Separation and Purification Technology,* 72(1), 28-33. https://doi.org/10.1016/j.seppur.2010.01.002
21. Matsumoto, T., Tatsumi, D., Tamai, N., & Takaki, T. (2001). Solution properties of celluloses from different biological origins in LiCl · DMAc. *Cellulose,* 8(4), 275-282. 10.1023/A:1015162027350
22. Niu, X., Huan, S., Li, H., Pan, H., & Rojas, O. J. (2021). Transparent films by ionic liquid welding of cellulose nanofibers and polylactide: Enhanced biodegradability in marine environments. *Journal of Hazardous Materials,* 402, 124073. https://doi.org/10.1016/j.jhazmat.2020.124073
23. Nunes, S. P., Culfaz-Emecen, P. Z., Ramon, G. Z., Visser, T., Koops, G. H., Jin, W., & Ulbricht, M. (2020). Thinking the future of membranes: Perspectives for advanced and new membrane materials and manufacturing processes. *Journal of Membrane Science,* 598, 117761. https://doi.org/10.1016/j.memsci.2019.117761
24. Pang, J., Wu, M., Zhang, Q., Tan, X., Xu, F., Zhang, X., & Sun, R. (2015). Comparison of physical properties of regenerated cellulose films fabricated with different cellulose feedstocks in ionic liquid. *Carbohydrate Polymers,* 121, 71-78. https://doi.org/10.1016/j.carbpol.2014.11.067
25. Patil, P. P., Reagan, M. R., & Bohara, R. A. (2020). Silk fibroin and silk-based biomaterial derivatives for ideal wound dressings. *International Journal of Biological Macromolecules,* 164, 4613-4627. https://doi.org/10.1016/j.ijbiomac.2020.08.041
26. Qi, H., Cai, J., Na, N., & Kuga, S. (2009). Properties of Films Composed of Cellulose Nanowhiskers and a Cellulose Matrix Regenerated from Alkali/Urea Solution. *Biomacromolecules,* 10, 1597-1602. 10.1021/bm9001975
27. Qi, Y., Lin, S., Lan, J., Zhan, Y., Guo, J., & Shang, J. (2021). Fabrication of super-high transparent cellulose films with multifunctional performances via postmodification strategy. *Carbohydrate Polymers,* 260, 117760. https://doi.org/10.1016/j.carbpol.2021.117760
28. Rabideau, B. D., & Ismail, A. E. (2015). Effect of Water Content in N-Methylmorpholine N-Oxide/Cellulose Solutions on Thermodynamics, Structure, and Hydrogen Bonding. *The Journal of Physical Chemistry B,* 119(48), 15014-15022. 10.1021/acs.jpcb.5b07500
29. Raghuwanshi, V. S., & Garnier, G. (2019). Cellulose Nano-Films as Bio-Interfaces. *Frontiers in Chemistry,* 7(535). 10.3389/fchem.2019.00535
30. Reuvers, A. J., & Smolders, C. A. (1987). Formation of membranes by means of immersion precipitation: Part II. the mechanism of formation of membranes prepared from the system cellulose acetate-acetone-water. *Journal of Membrane Science,* 34(1), 67-86. https://doi.org/10.1016/S0376-7388(00)80021-6
31. Reuvers, A. J., van den Berg, J. W. A., & Smolders, C. A. (1987). Formation of membranes by means of immersion precipitation: Part I. A model to describe mass transfer during immersion precipitation. *Journal of Membrane Science,* 34(1), 45-65. https://doi.org/10.1016/S0376-7388(00)80020-4

32. Samir, A., Said, M. A., Alloin, F., & Dufresne, A. (2005). Review of Recent Research into Cellulosic Whiskers, Their Properties and Their Application in Nanocomposite Field. *Biomacromolecules,* 6(2), 612-626. 10.1021/bm0493685
33. Sayyed, A. J., Deshmukh, N. A., & Pinjari, D. V. (2019). A critical review of manufacturing processes used in regenerated cellulosic fibres: viscose, cellulose acetate, cuprammonium, LiCl/DMAc, ionic liquids, and NMMO based lyocell. *Cellulose,* 26(5), 2913-2940. 10.1007/s10570-019-02318-y
34. Shahbazi, H., Tataei, M., Enayati, M. H., Shafeiey, A., & Malekabadi, M. A. (2019). Structure-transmittance relationship in transparent ceramics. *Journal of Alloys and Compounds,* 785, 260-285. https://doi.org/10.1016/j.jallcom.2019.01.124
35. Shandilya, M., Thakur, S., & Thakur, S. (2020). Magnetic amendment in the fabrication of environment friendly and biodegradable iron oxide/ethyl cellulose nanocomposite membrane via electrospinning. *Cellulose,* 27(17), 10007-10017. 10.1007/s10570-020-03455-5
36. Shi, S., Zhu, K., Chen, X., Hu, J., & Zhang, L. (2019). Cross-Linked Cellulose Membranes with Robust Mechanical Property, Self-Adaptive Breathability, and Excellent Biocompatibility. *ACS Sustainable Chemistry & Engineering,* 7(24), 19799-19806. 10.1021/acssuschemeng.9b05092
37. Swatloski, R. P., Spear, S. K., & Holbrey, J. D. (2002). Dissolution of cellulose [correction of cellose] with ionic liquids. *Journal of the American Chemical Society,* 124(18), 4974-4975. https://doi.org/10.1021/ja025790m
38. Tang, C., & Liu, H. (2008). Cellulose nanofiber reinforced poly(vinyl alcohol) composite film with high visible light transmittance. *Composites Part A: Applied Science and Manufacturing,* 39(10), 1638-1643. https://doi.org/10.1016/j.compositesa.2008.07.005
39. Tehrani-Bagha, & Reza, A. (2019). Waterproof breathable layers – A review. *Advances in Colloid and Interface Science,* 268, 114-135. https://doi.org/10.1016/j.cis.2019.03.006
40. Trygg, J., & Fardim, P. (2011). Enhancement of cellulose dissolution in water-based solvent via ethanol–hydrochloric acid pretreatment. *Cellulose,* 18(4), 987-994. 10.1007/s10570-011-9550-y
41. van de Witte, P., Dijkstra, P. J., van den Berg, J. W. A., & Feijen, J. (1996). Phase separation processes in polymer solutions in relation to membrane formation. *Journal of Membrane Science,* 117(1), 1-31. https://doi.org/10.1016/0376-7388(96)00088-9
42. Wan, J., Diao, H., Yu, J., Song, G., & Zhang, J. (2021). A biaxially stretched cellulose film prepared from ionic liquid solution. *Carbohydrate Polymers,* 260, 117816. https://doi.org/10.1016/j.carbpol.2021.117816
43. Wang, C., Shi, J., He, M., Ding, L., Li, S., Wang, Z., & Wei, J. (2018). High strength cellulose/ATT composite films with good oxygen barrier property for sustainable packaging applications. *Cellulose,* 25(7), 4145-4154. 10.1007/s10570-018-1855-7
44. Wang, Y., Yuan, L., Tian, H., Zhang, L., & Lu, A. (2019). Strong, transparent cellulose film as gas barrier constructed via water evaporation induced dense packing. *Journal of Membrane Science,* 585, 99-108. https://doi.org/10.1016/j.memsci.2019.04.059

45. Xie, W., Li, T., Tiraferri, A., Drioli, E., Figoli, A., Crittenden, J. C., & Liu, B. (2021). Toward the Next Generation of Sustainable Membranes from Green Chemistry Principles. *ACS Sustainable Chemistry & Engineering,* 9(1), 50-75. 10.1021/acssuschemeng.0c07119
46. Xu, Z., Liao, J., Tang, H., Efome, J. E., & Li, N. (2018). Preparation and antifouling property improvement of Tröger's base polymer ultrafiltration membrane. *Journal of Membrane Science,* 561, 59-68. https://doi.org/10.1016/j.memsci.2018.05.042
47. Yan, C., Wang, R., Wan, J., Zhang, Q., Xue, S., Wu, X., Cong, W. (2016). Cellulose/microalgae composite films prepared in ionic liquids. *Algal Research,* 20, 135-141. https://doi.org/10.1016/j.algal.2016.09.024
48. Yaopeng, Z., Huili, S., xinyuan, S., & Xuechao, H. (2002). Morphology ,permeation and cutoff properties of cellulose membranes prepared by NMMO method. *Membrane Science And Technology*(04), 13-20-25.
49. Yuan, W., Wu, K., Liu, N., Zhang, Y., & Wang, H. (2018). Cellulose acetate fibers with improved mechanical strength prepared with aqueous NMMO as solvent. *Cellulose,* 25(11), 6395-6404. 10.1007/s10570-018-2032-8
50. Yue, Y., Gong, X., Jiao, W., Li, Y., Yin, X., Si, Y., Ding, B. (2021). In-situ electrospinning of thymol-loaded polyurethane fibrous membranes for waterproof, breathable, and antibacterial wound dressing application. *Journal of Colloid and Interface Science,* 592, 310-318. https://doi.org/10.1016/j.jcis.2021.02.048
51. YukinobuFukaya, KensakuHayashi, & MasahisaWada. (2008). Cellulose dissolution with polar ionic liquids under mild conditions: required factors for anions. *Green chemistry,* 10(1), 44-46. 10.1039/B713289A
52. Yuping, Z., & Xiao, C. (2010). Discussion on Crystallinity Calculated by the Technology of Peak Separation. *Research And Exploration In Laboratory,* 29(03), 41-43.
53. Zhang, L., Zhou, J., & Zhang, L. (2013). Structure and properties of β-cyclodextrin/cellulose hydrogels prepared in NaOH/urea aqueous solution. *Carbohydrate Polymers,* 94(1), 386-393. https://doi.org/10.1016/j.carbpol.2012.12.077
54. Zhang, Y. (2002). Preparation and Formation Mechanism of Cellulose Membranes Prepared form NMMO Solution. Dong Hua University.
55. Zhang, Y., Tian, Z., Fu, Y., Wang, Z., Qin, M., & Yuan, Z. (2020). Responsive and patterned cellulose nanocrystal films modified by N-methylmorpholine-N-oxide. *Carbohydrate Polymers,* 228, 115387. https://doi.org/10.1016/j.carbpol.2019.115387
56. Zhang, Y., Tong, X., Zhang, B., Zhang, C., Zhang, H., & Chen, Y. (2018). Enhanced permeation and antifouling performance of polyvinyl chloride (PVC) blend Pluronic F127 ultrafiltration membrane by using salt coagulation bath (SCB). *Journal of Membrane Science,* 548, 32-41. https://doi.org/10.1016/j.memsci.2017.11.003
57. Zheng, B., Luo, Y., Liao, H., & Zhang, C. (2017). Investigation of the crystallinity of suspension plasma sprayed hydroxyapatite coatings. *Journal of the European Ceramic Society,* 37(15), 5017-5021.

https://doi.org/10.1016/j.jeurceramsoc.2017.07.007

58. Zheng, X., Huang, F., Chen, L., Huang, L., Cao, S., & Ma, X. (2019). Preparation of transparent film via cellulose regeneration: Correlations between ionic liquid and film properties. *Carbohydrate Polymers,* 203, 214-218. https://doi.org/10.1016/j.carbpol.2018.09.060
59. Zhou, Z., Ma, J., Li, K., Zhang, W., Li, K., Tu, X., . . . Zhang, H. (2021). A Plant Leaf-Mimetic Membrane with Controllable Gas Permeation for Efficient Preservation of Perishable Products. *ACS Nano.* 10.1021/acsnano.1c00997
60. Zhu, K., Shi, S., Cao, Y., Lu, A., Hu, J., & Zhang, L. (2019). Robust chitin films with good biocompatibility and breathable properties. *Carbohydrate Polymers,* 212, 361-367. https://doi.org/10.1016/j.carbpol.2019.02.054

Figures

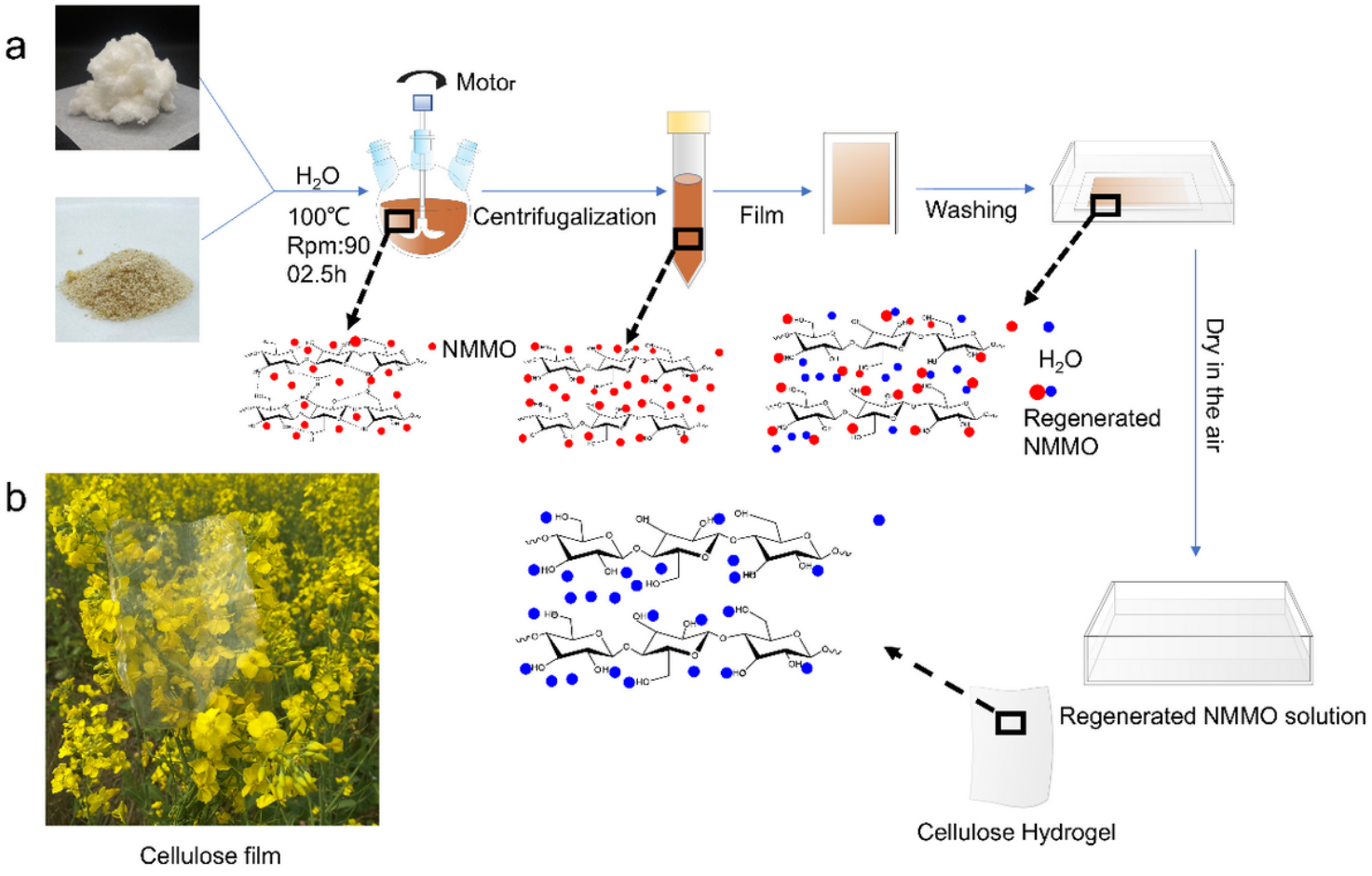

Figure 1

Preparation process of cellulose film: (a) The process. (b) The cellulose dry film.

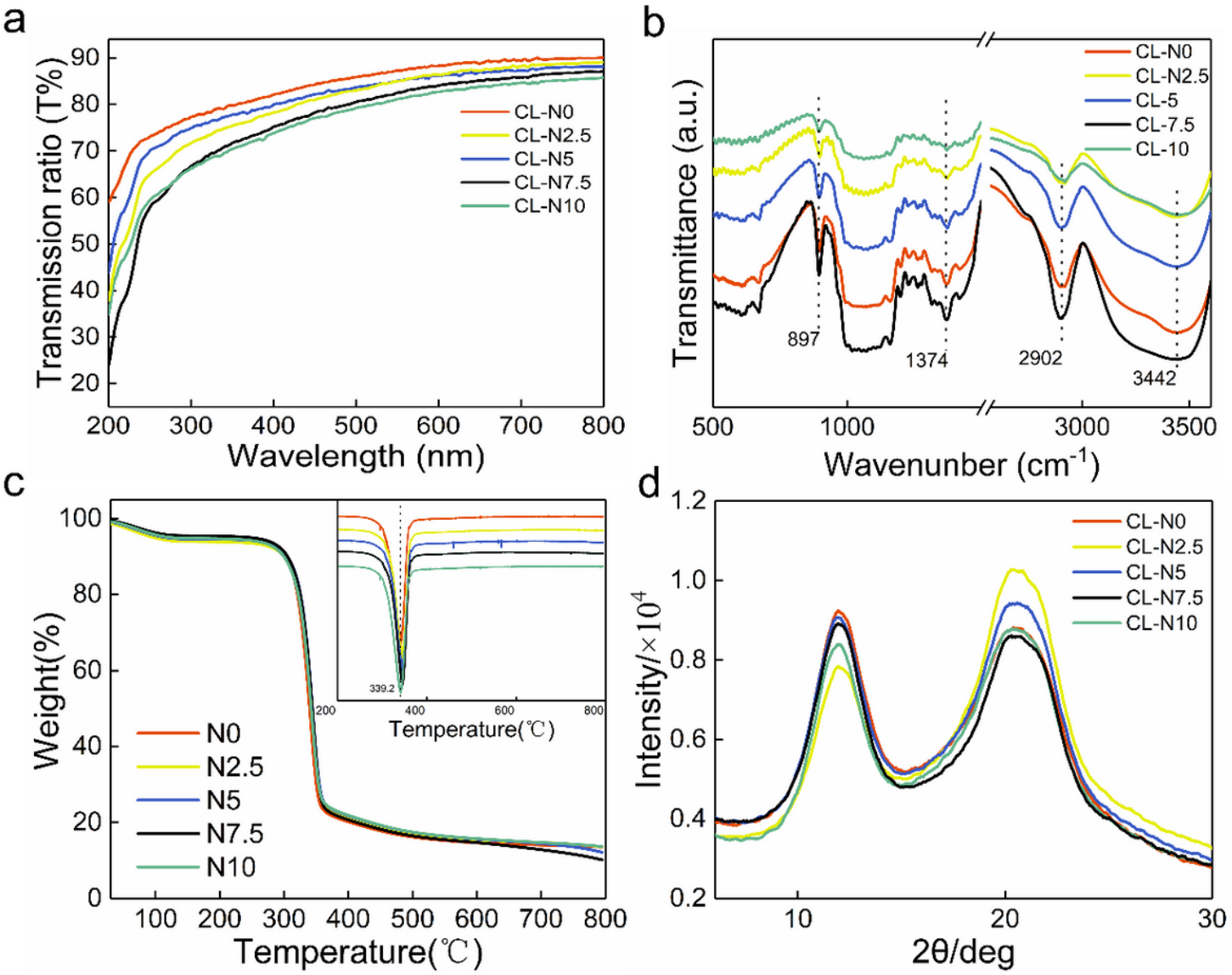

Figure 2

Characteristics of CL-N series films: (a) The optical transmittance curves, (b) FTIR spectrum, (c) TG and DTG, (d) X-ray diffraction (XRD) patterns of the CL-N series film.

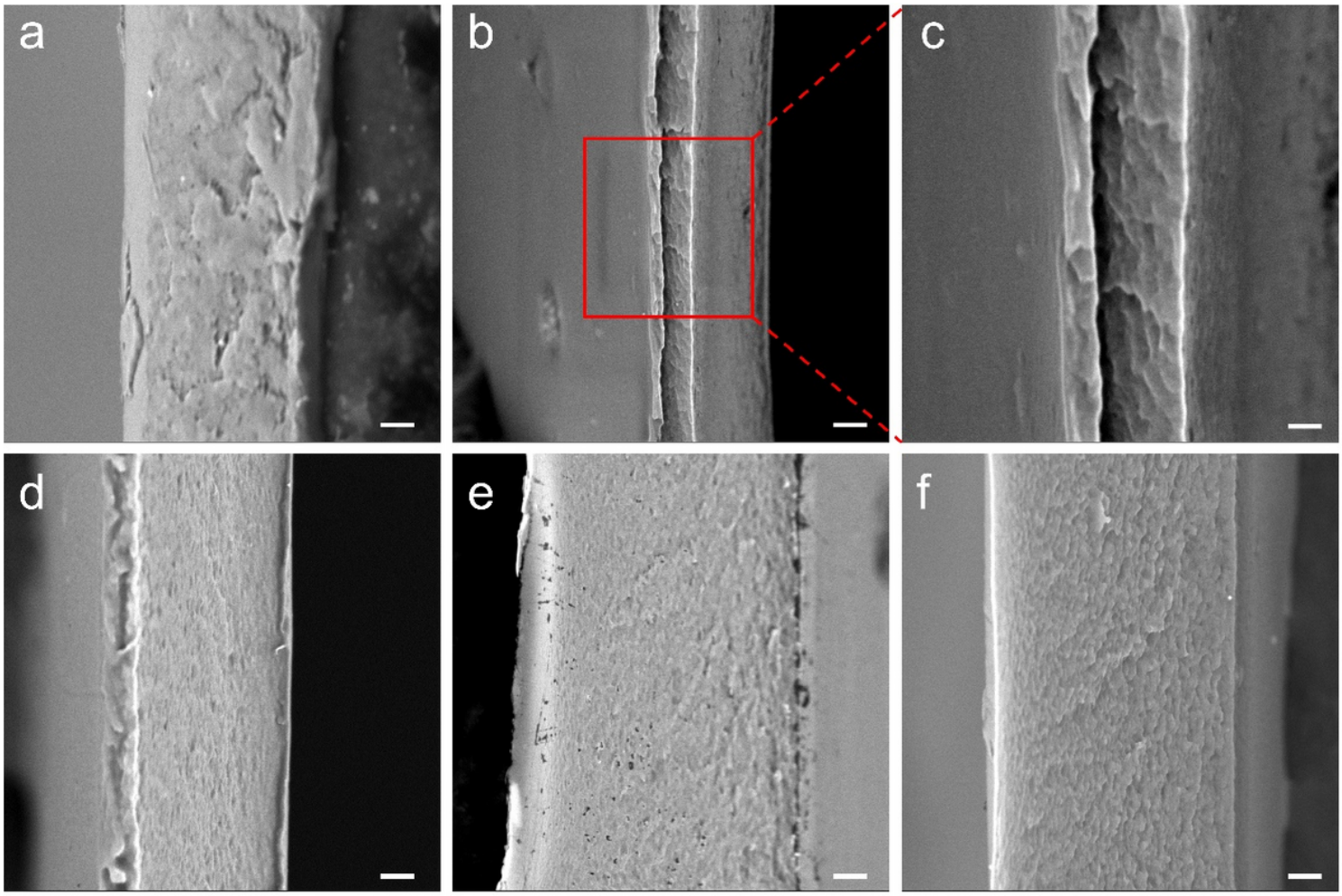

Figure 3

SEM images of the CL-N series film: (a) CL-N0, (b-c) CL-N2.5, (d) CL-N5, (e) CL-N7.5, (f) CL-N10. Except for image c (0.69μm), all other image scale bar corresponds to 2μm.

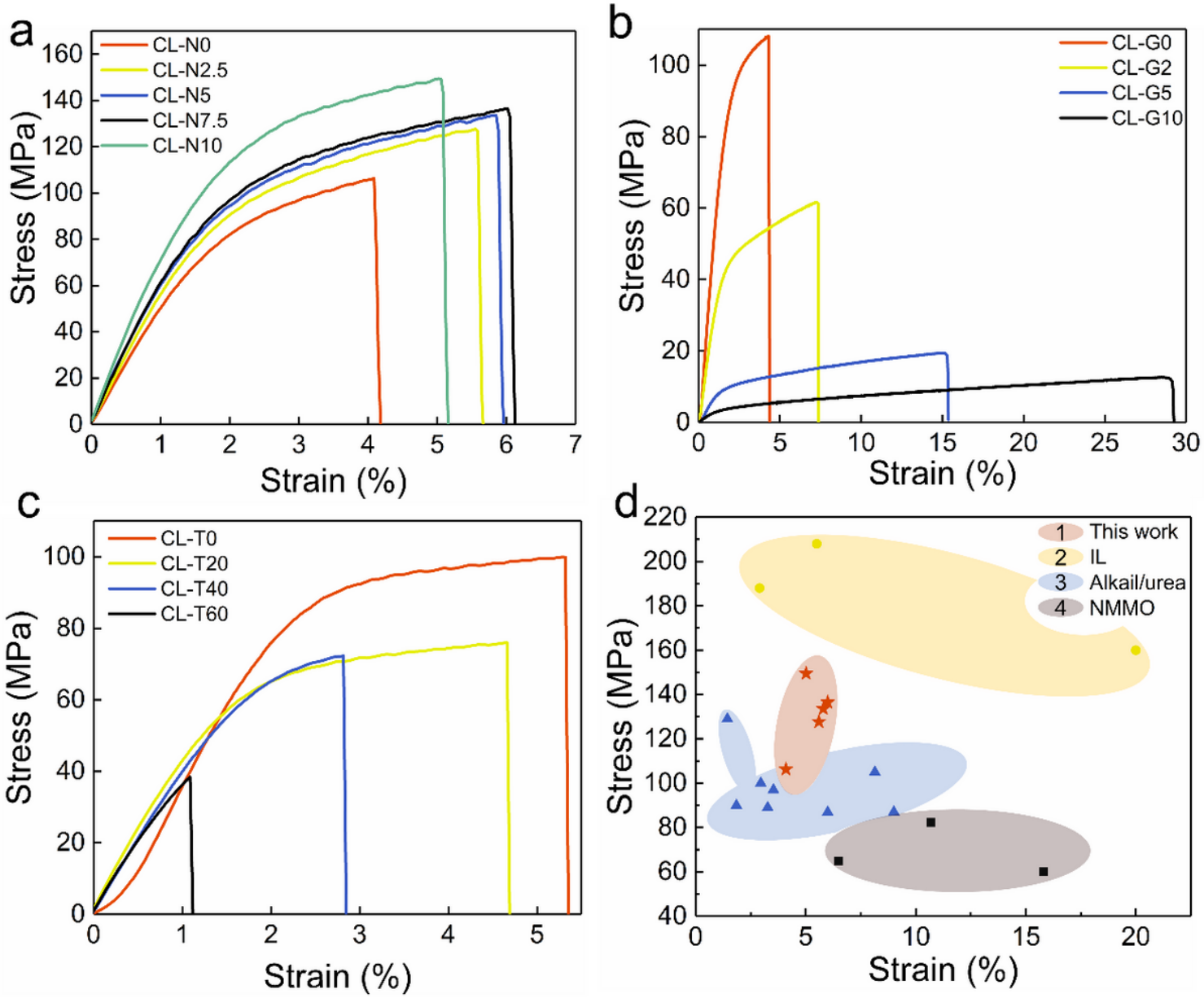

Figure 4

Mechanical properties of the cellulose film: (a) CL-N series film, (b) CL-G series film, (c) CL-T series film and (d)mechanical property of CL-N series film compared with other regenerated cellulose films. Oval 1 represents the CL-N series film from NMMO/H2O system in this work. Ovals 2-4 represent the regenerated cellulose film from ionic liquid(Wan et al., 2021; X. Zheng et al., 2019; Yan et al., 2016; Pang et al., 2015), Alkali/Urea aqueous system(Shi et al., 2019; Liu et al., 2019; C. Wang et al., 2018; H. Qi et al., 2009), NMMO/H2O(Kim et al., 2011; Mao et al., 2010; Khare et al., 2007), respectively. The scattering points in the figure are the values of the mechanical properties data of cellulose fibers reported in references.

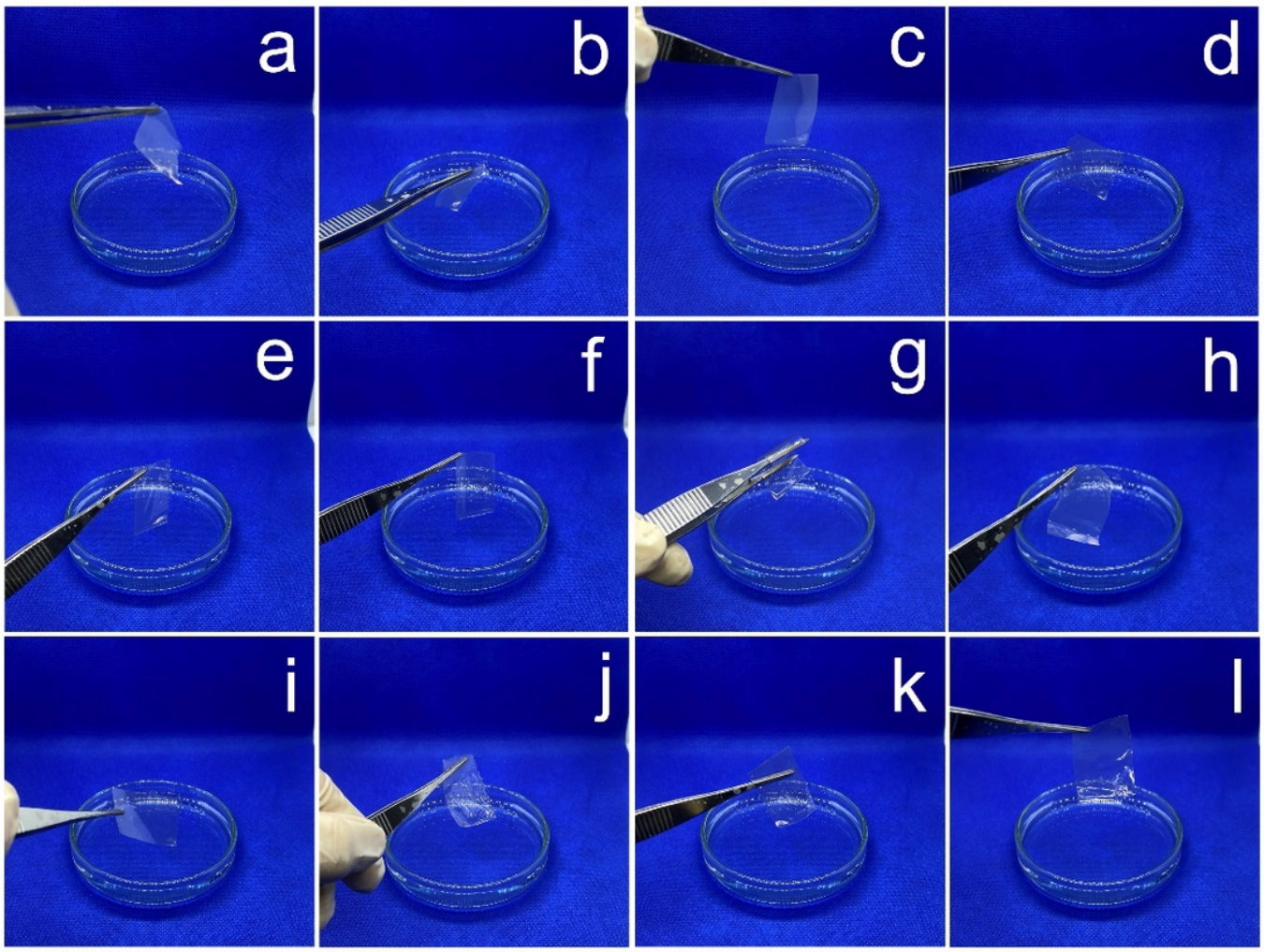

Figure 5

Solvent resistance test of CL-N0: (a) water, (b) acid solution(pH=1), (c) alkali solution (pH = 13), (d) acetone, (e) methanol, (f) ethanol, (g) DMAC, h Petroleum ether, (i) THF, (j) ethyl acetate, (k) toluene, (l) acetonitrile. All the above tests are carried out in a 250ml glass beaker, and the immersion time of the CL-N0 in different solutions is 24 hours.

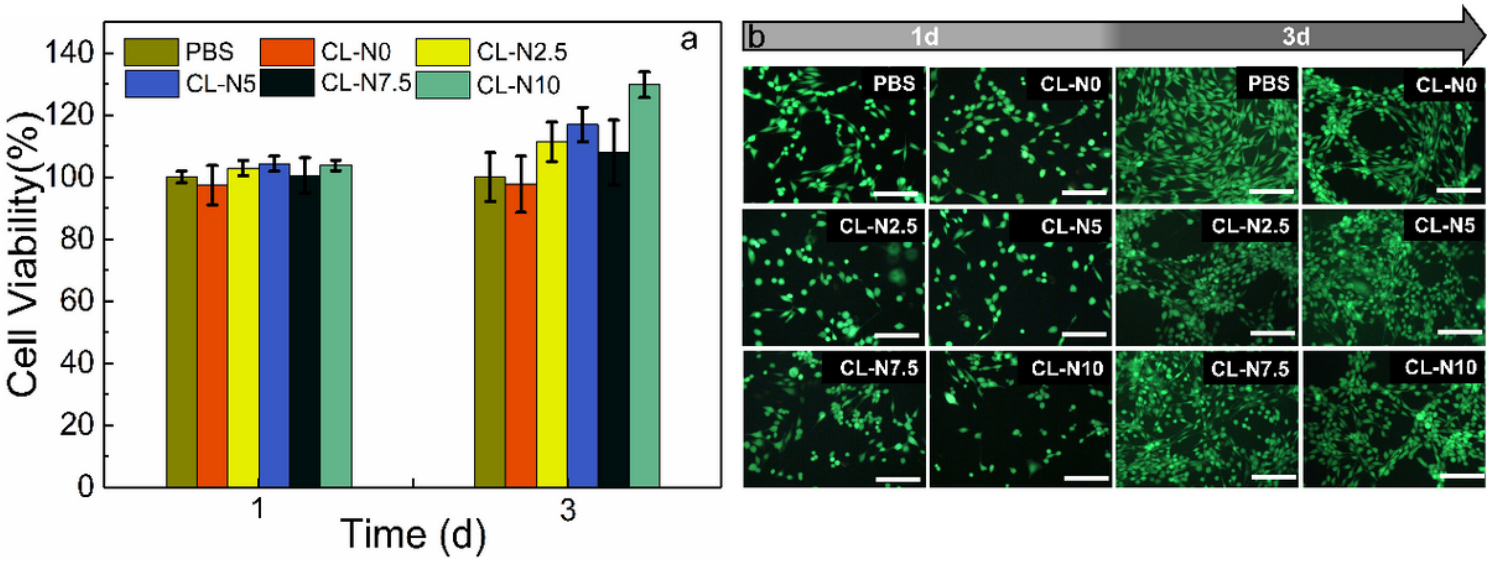

Figure 6

Cytotoxicity and biological compatibility of CL-N series film: (a) Cell viability of NIH-3T3 cells incubated with CL-N series film (CCK-8 assay, mean ± SD). (b) Fluorescence microscopic images of NIH-3T3 cells cultured with CL-N series film stained with Live–Dead assay (green/red, respectively) after 24 h and 72 h culture. Scale bar: 100 μm.

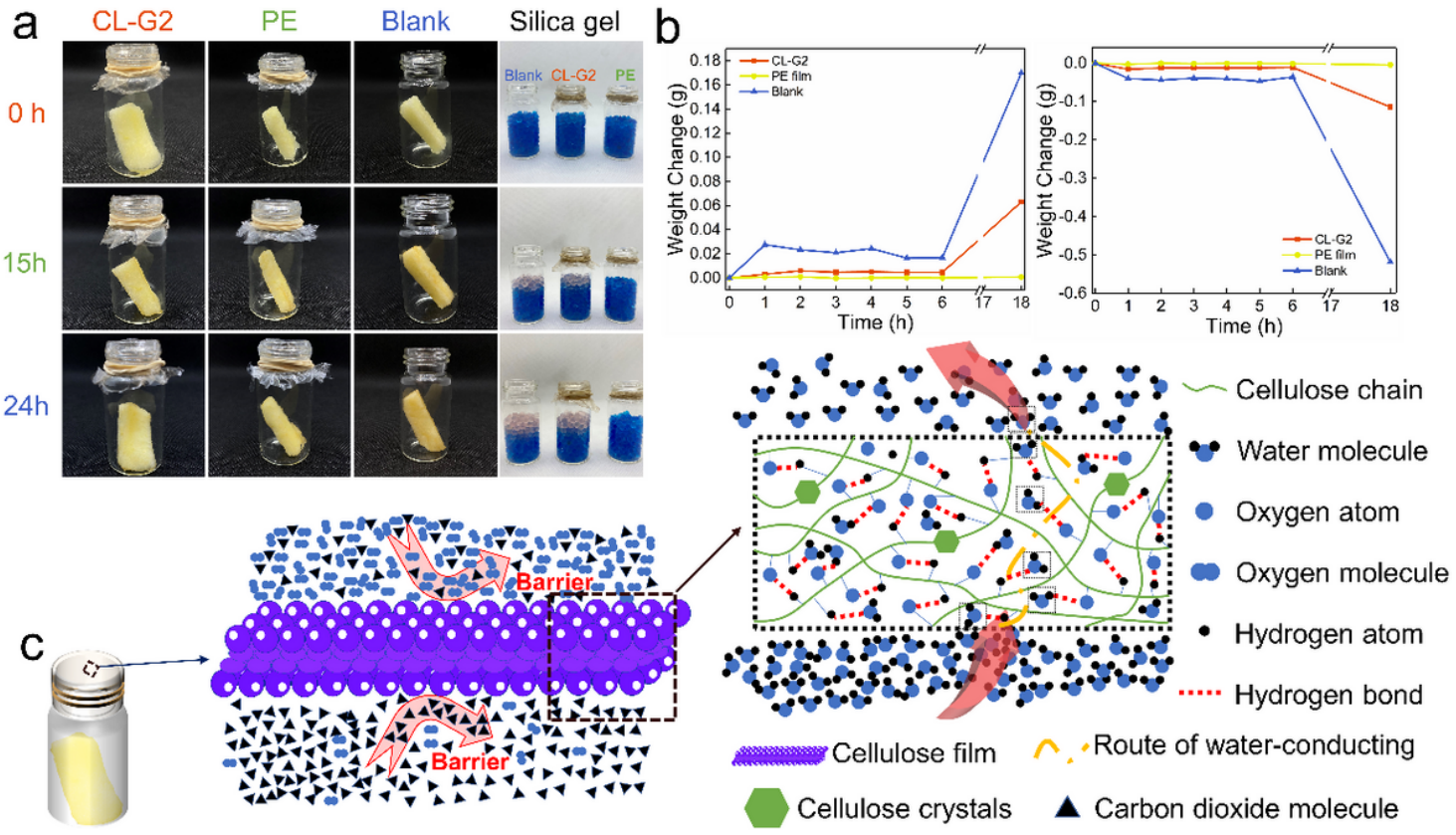

Figure 7

Moisture-conducting and air barrier properties: (a) the color change of silica gel and apple recorded at 0, 15 and 24h respectively, (b) apple group and silica gel group weight change over time, (c) the mechanism of moisture-conducting and air barrier properties.